Study of surface morphology and inhibition efficiency of mild steel in simulated concrete pore solution by lactic acid–Zn^{2+} system

P.N. Devi,[1] J. Sathiyabama[1] and S. Rajendran[1,2]

[1] *PG and Research Department of Chemistry, GTN Arts College, Dindigul-624005, India*
[2] *Corrosion Research Centre, Department of Chemistry, St Antony's College of Arts and Sciences for Women, Amala Annai Nagar, Thamaraipadi (Post), Dindigul – 624 005, Tamilnadu, India*
E-mail: susairajendran@gmail.com

Abstract

The inhibition efficiency (*IE*) of lactic acid–Zn^{2+} system in controlling corrosion of mild steel in simulated concrete pore solution (SCPS) prepared in well water in the absence and presence of Zn^{2+} has been investigated by weight loss study. The formulation consisting of 250 ppm of lactic acid and 50 ppm of Zn^{2+} provides 94% of inhibition efficiency. Inhibition was found to increase with an increasing concentration of lactic acid and Zn^{2+}. Polarization resistance was measured by weight loss method, polarization study. The surface morphology has been investigated by SEM and AFM.

Introduction

The corrosion of concrete steel reinforcement is a major issue that concerns not only the civil engineering industry but also other areas such as the nuclear industry. Due to the alkalinity of the interstitial solution (pH 13), steel reinforcements remain passive. Long term exposure to environmental actions (chemical, biological and physical effects of the environment), causes deterioration of concrete and reinforcement. When considering the reliability of structures all type of actions should be taken into accounts. This holistic approach to the design and verification of structures shall be applied to all constructions especially civil engineering works, because of their larger ratio between the area exposed to the surrounding environment and cross-section dimensions as well as longer design life [1].

Metals are extracted from their ores by reduction process. When metals come in contact with the environment, especially oxygen and moisture, they deteriorate. This process, we call corrosion. Corrosion is the desire of pure metals to go back to its original state of ores. Corrosion is a natural, spontaneous and thermodynamically stable process. The process of corrosion can be controlled but it cannot be prevented. Carbon steel

reinforcements in concrete structures are in passive conditions that they are protected by a thin oxide layer promoted by the concrete alkalinity. Corrosion can initiate only when passivity is destroyed. This occurs in two ways: carbonation of concrete, the reaction of atmospheric CO_2 with cement paste, that lowers pH and causes general corrosion; the presence of chlorides at the steel surface in concentration higher than a critical threshold, generally considered in the range of 0.4−1% by a cement weight [2]. Among available methods, corrosion inhibitors seem to be attractive because of their low cost and easy handling, compared with other preventive methods. Inhibitors can be divided in two groups: admixed inhibitors, added to fresh concrete for new structures, and migrating inhibitors, which can penetrate into the hardened concrete and are usually proposed in repair systems. While admixed inhibitors are commercially available since 70's, migrating corrosion inhibitors for concrete structures were proposed in the last 15−20 years [3]. Nowadays, there are several admixtures available on the market: inorganic compounds based on nitrites, especially used as additives [4−8] and sodium monofluorophosphate used as migrating inhibitors [9, 10], organic compounds based on mixtures of alkanolamines, amines or amino acids, or based on an emulsion of unsaturated fatty acid, proposed both as admixed and migrating inhibitor [11]. Other non commercial inhibitors, both inorganic and organic were studied: zinc oxide [12], molybdates and borates [13], stannates [14], carboxylate ions, quaternary ammonium salts and many other organic compounds [15]. The present work is undertaken:

1. To evaluate the inhibition efficiency and the corrosion resistance by weight loss method and electrochemical studies.
2. To study of the surface morphology by FTIR, scanning electron microscopy (SEM) and atomic force microscope (AFM).

Experimental section

Preparation of simulated concrete pore solution (SCPS)

Simulated concrete pore solution mainly consists of saturated $Ca(OH)_2$, KOH, and NaOH with the pH 13.5 [16]. However in numerous studies of rebar corrosion, saturated $Ca(OH)_2$ has been used a substitute for pore solution. Saturated calcium hydroxide solution is used in present study, as simulated concrete pore solution with the pH 12.5.

Preparation of the specimens

Metal specimens of the dimensions $1 \times 4 \times 0.2$ cm were polished to a mirror finish and degreased with acetone. Then they were used for the weight-loss method and surface examination studies. The environment chosen is well water and the physico-chemical parameters of well water are given in Table 1.

Table 1. Physicochemical parameters of well water.

Parameters	Value
pH	8.38
Conductivity	1770 $\mu\Omega^{-1}$ cm^{-1}
Chloride	665 ppm
Sulphate	214 ppm
TDS	1100 ppm
Total hardness	402 ppm
Total alkalinity	390 ppm
Magnesium	83 ppm
Potassium	55 ppm
Sodium	172 ppm
Calcium	88 ppm

Determination of Corrosion Rate

The weighed specimens in triplicate were suspended by means of glass hooks in 100 ml SCPS prepared in well water containing various concentration of lactic acid in the presence and absence of Zn^{2+} for one day. The specimen were taken out, washed in running water, dried, and weighed. From the change in weights of the specimens, corrosion rates were calculated using the following relationship:

$CR=$[(Weight loss in mg)/(Area of specimens in dm^2×Immersion period in days)] mdd (1)

Corrosion inhibition efficiency (*IE*, %) was then calculated using the equation:

$$IE = 100[1-(W_2/W_1)] \% \tag{2}$$

Where, W_1 = corrosion rate in the absence of the inhibitors, and W_2 = corrosion rate in the presence of the inhibitors.

Potentiodynamic Polarization

Polarization studies were carried out in a CHI – Electrochemical workstation with impedance, Model 660A. A three-electrode cell assembly was used. The three electrode assembly is shown in Figure 1. The working electrode was mild steel. A saturated calomel electrode (SCE) was the reference electrode and platinum was the counter electrode. From the polarization study, corrosion parameters such as corrosion potential (E_{corr}), corrosion current (I_{corr}) and Tafel slopes (anodic = b_a and cathodic = b_c) and Linear polarization resistance (LPR) were calculated. The scan rate (V/s) was 0.01. Hold time at (E_{fcs}) was zero and quit time (s) was two.
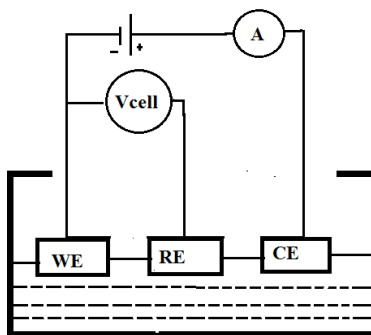
Figure 1. Circuit diagram of three-electrode cell assembly.

Fourier Transform Infrared Spectra

These spectra were recorded in a Perkin-Elmer 1600 spectrometer using KBr pellets. The spectrum of the protective film was recorded by carefully removing the film, mixing it with KBr and making the pellet.

Scanning Electron Microscopic Studies (SEM)

The carbon steel immersed in blank solution and in the inhibitor solution for a period of one day was removed, rinsed with double-distilled water, dried, and observed in a scanning electron microscope to examine the surface morphology. The surface morphology measurements of carbon steel were examined using JEOL MODEL6390 computer-controlled scanning electron microscope.

Atomic Force of Microscopy

The mild steel specimens were immersed in blank and in the inhibitor solution for a period of one day. The specimens were removed, rinsed with double distilled water, dried and subjected to the surface examination. Atomic force microscopy (Veeco Innova model) was used to observe the samples surface in tapping model, using cantilever with linear tips. The scanning area in the images was 50 µm × 50 µm and the scan rate was 1 µm/s.

Results and Discussion

Analysis of Weight loss Study

Corrosion rates of carbon steel immersed in SCPS prepared in well water in the absence and presence of inhibitors (lactic acid and Zn^{2+} system) were calculated. The calculated corrosion inhibition efficiency (*IE)* and corrosion rates (*CR*) of lactic acid in controlling corrosion of SCPS in well water, for a period of one day in absence and presence of zinc ion are given in Table 2 and represented in Figure 2. It is observed from the Table 2 that lactic acid is a good inhibitor. The *IE* is found to be enhanced in the presence of Zn^{2+} ion. Lactic acid alone shows some inhibition efficiencies. The formulation consisting of 250 ppm of lactic acid and 50 ppm of Zn^{2+} shows 94% of inhibition efficiency. Weight loss

study reveals that lactic acid and Zn^{2+} individually showed some *IE*, but exhibited better *IE* when applied in combination. This suggests that LA and Zn^{2+} exhibit synergistic behaviour [17–20].

Table 2. Corrosion rates (*CR*) of mild steel immersed in simulated concrete pore solution (SCPS) prepared in well water in the presence and absence of lactic acid Zn^{2+} in the inhibition efficiency (IE) obtained by weight loss method.

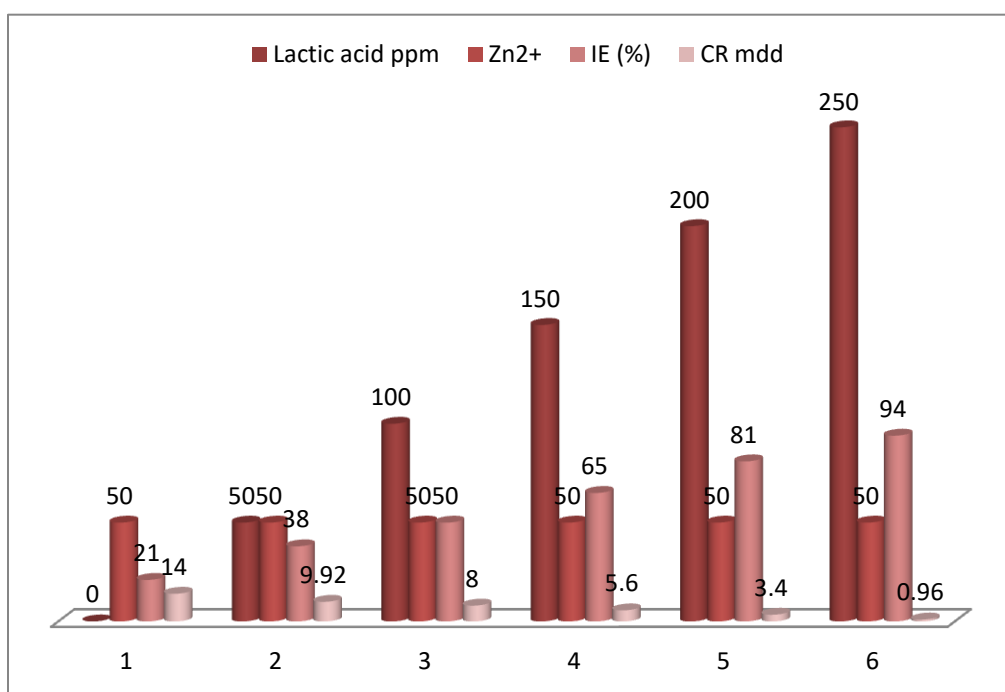| Lactic acid ppm	Zn^{2+} (0 ppm)		Zn^{2+} (25 ppm)		Zn^{2+} (50 ppm)	
	IE%	*CR*, mdd	*IE%*	*CR*, mdd	*IE%*	*CR*, mdd
0	–	16	17	13.2	21	14.0
50	19	12.96	31	11.04	38	9.92
100	25	12.00	38	9.92	50	8.00
150	36	10.24	40	9.60	65	5.60
200	44	8.96	50	8.00	81	3.40
250	63	5.92	75	4.00	94	0.96

Figure 2. Corrosion rates (*CR*) and inhibition efficiency (*IE*) of lactic acid–Zn^{2+} system in the corrosion of mild steel immersed in simulated concrete pore solution (SCPS) prepared in well water.

Analysis of Polarization Curves

When mild steel is immersed in simulated concrete pore solution prepared in well water the corrosion potential was -842 mV *vs* SCE (Figure 3). When lactic acid (250 ppm) and Zn^{2+} (50 ppm) are added to the above system the corrosion potential shifted to the anodic side -774 mV *vs* SCE; that is noble side. This indicates that the $LA-Zn^{2+}$ system controls anodic reaction predominantly. It is inferred that a passive film is formed on the metal surface in presence of inhibitor. The shifting of corrosion potential towards anodic side in presence of inhibitors has been reported by several researchers [21–24].
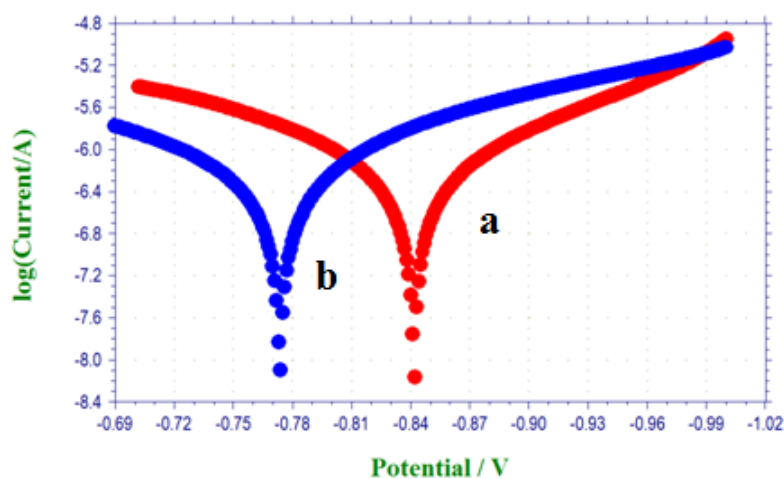

Figure 3. Polarization curves of mild steel immersed in various test solution: a) SCPS ; b) lactic acid 250 ppm + Zn^{2+} 50 ppm.

Further, the LPR value increases from 41473 Ohm cm^2 to 47099 Ohm cm^2; the corrosion current decreases from $7.237 \cdot 10^{-7}$ A/cm^2 to $5.768 \cdot 10^{-7}$ A/cm^2. When a passive film formed on mild steel surface, in presence of inhibitor system the electron transfer from the metal surface towards the bulk of the solution is difficult and prevented. So rate of corrosion decreases and hence corrosion current decreases in presence of inhibitor system.

Table 3. Corrosion parameters of mild steel immersed in SCPS prepared in well water in the absence and presence of inhibitor system obtained from Potentiodynamic Polarization Study.

System	E_{corr} mV *vs* SCE	b_c mV/ decade	b_a mV/decade	LPR Ohm cm^2	I_{corr} A/cm^2
SCPS	-842	131	145	41473	$7.237 \cdot 10^{-7}$
SCPS + lactic acid 250 ppm + Zn^{2+} 50ppm	-774	171	213	47099	$5.768 \cdot 10^{-7}$

Analysis of AC Impedance spectra

AC impedance spectra (electrochemical impedance spectra) have been used to confirm the formation of protective film on the metal surface. If a protective film is formed on the metal surface, charge transfer resistance decreases and the impedance log (z/ohm) value increases [25, 26]. The AC impedance spectra of mild steel immersed in SCPS prepared in well water in the absence and presence of inhibitors (LA–Zn^{2+}) are shown in Figure 4 (Nyquist plots) and Figures 5a and 5b (Bode plots). The AC impedance parameters namely charge transfer resistance (R_t) and double layer capacitance (C_{dl}) derived from Nyquist plots are given in Table 4. The impedance log (z/ohm) values derived from Bode plots are also given in Table 4.

Table 4. Corrosion parameters of mild steel immersed in SCPS prepared in well water in the absence and presence of inhibitor system obtained from AC impedance spectra.

System	Nyquist plot		Bode plot
	R_t, **Ohm cm^2**	C_{dl}, **F/cm^2**	**Impedance value** log (z/**Ohm**)
SCPS	566	$9.013 \cdot 10^{-9}$	2.86
SCPS + lactic acid 250 ppm + + Zn^{2+} 25 ppm	1385	$3.683 \cdot 10^{-9}$	3.28

It is observed that when the inhibitors lactic acid (250 ppm) + Zn^{2+} (50 ppm) are added to SCPS, the charge transfer resistance (R_t) increases from 566 Ohm cm^2 to 1385 Ohm cm^2. The C_{dl} value decreases from $9.013 \cdot 10^{-9}$ F/cm^2 to $3.683 \cdot 10^{-9}$ F/cm^2. The impedance values [log (z/ohm)] increases from 2.86 to 3.28. These results lead to the conclusion that a protective film is formed on the metal surface.
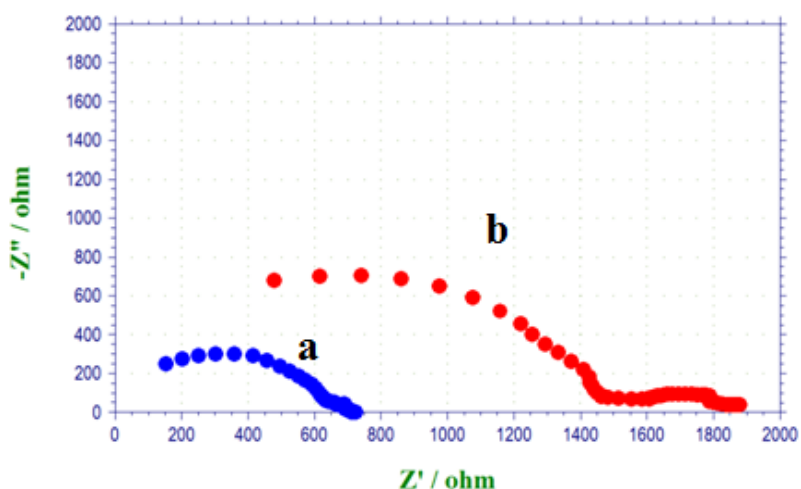

Figure 4. AC Impendence curves of mild steel immersed in various test solution (Nyquist plots): a) SCPS; b) SCPS + lactic acid 250 ppm + Zn^{2+} 50 ppm.
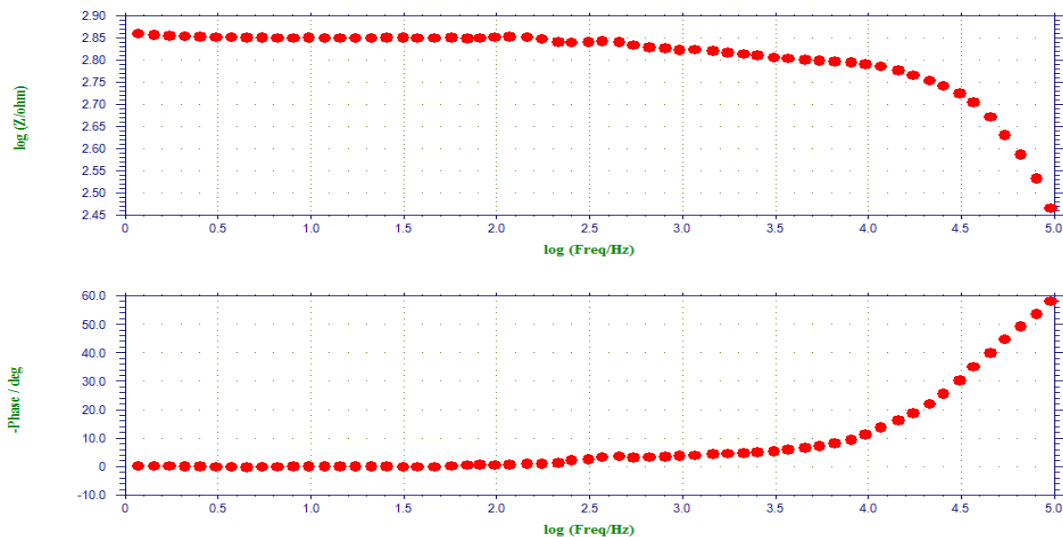
Figure 5(a). AC impendance spectra of mild steel immersed in SCPS (Bode plots).
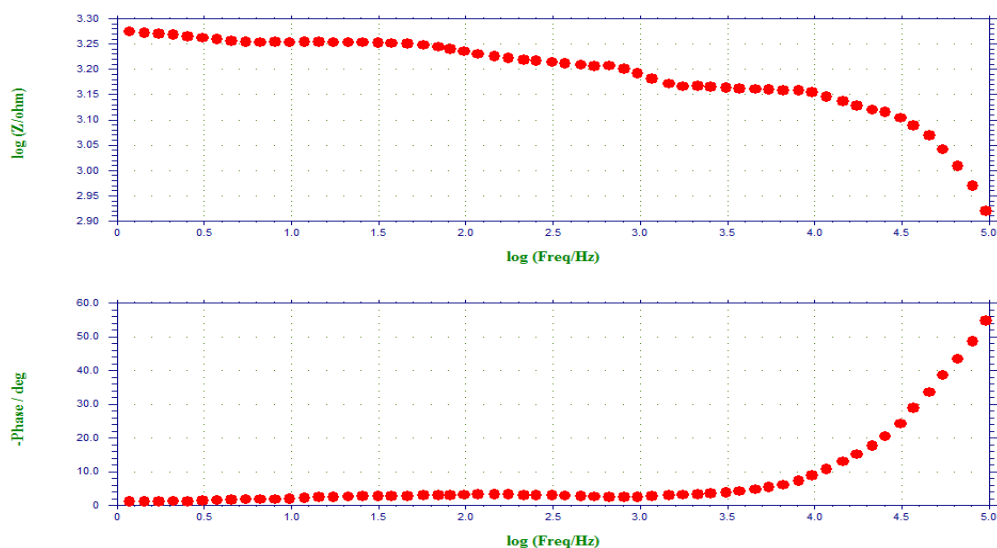

Figure 5(b). AC impendance spectrum of mild steel immersed in SCPS + 250 ppm lactic acid + 25 ppm Zn^{2+} system (Bode plots).

Analysis of FTIR spectra

The FTIR spectra were used to analyze the inhibitor film formed on mild steel. The FTIR spectrum of the pure lactic acid (Figure 6a) is compared with the FTIR spectrum of film formed on the metal surface after immersion in SCPS prepared in well water containing 250 ppm of lactic acid and 50 ppm of Zn^{2+} (Fig. 6b). The results showed that the OH stretching frequency of pure lactic acid appears at $3464 \, cm^{-1}$ where as in the SCPS containing 250 ppm of lactic acid and 50 ppm of Zn^{2+} system, the stretching frequency has shifted from $3464 \, cm^{-1}$ to $3358 \, cm^{-1}$. In case of C=O, the stretching frequency which appeared at $1733 \, cm^{-1}$ for lactic acid has disappeared for the SCPS system containing 250 ppm of lactic acid and 50 ppm of Zn^{2+} system. This confirms that the oxygen atom of

carboxyl group has coordinated with Fe^{2+} resulting in the formation of Fe^{2+}–lactic acid complex formed on the metal surface. And also, the peak appearing at 1435, 1024 and 693 cm^{-1} confirmed the presence of calcium carbonate, calcium oxide and calcium hydroxide formed on the metal surface [27, 28].
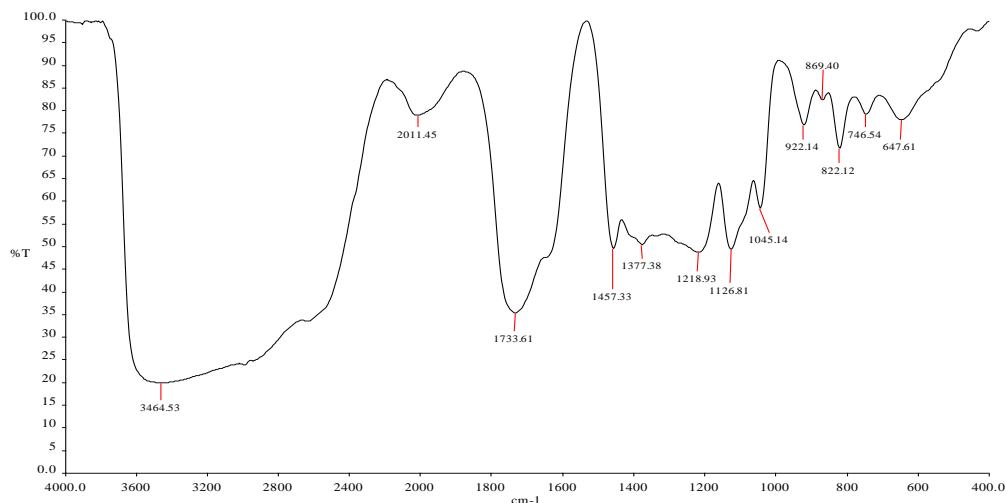
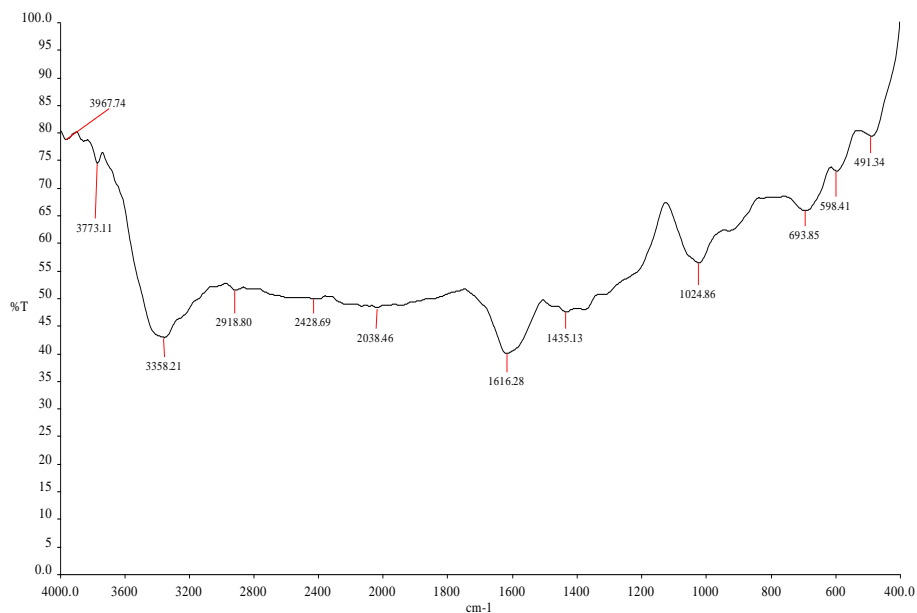**Figure 6(a).** FTIR spectrum of pure lactic acid.

Figure 6(b). FTIR spectrum of inhibitor film formed on the mild steel after immersion in SCPS prepared in well water containing of 250 ppm lactic acid and 50 ppm of Zn^{2+} .

Scanning Electron Microscopy(SEM)

Surface morphology of mild steel was studied by scanning electron microscopy after 24 h immersion in SCPS before and after addition of inhibitor. Figure 7(a) represent the micrograph obtained of polished steel without being exposed to the corrosive environment while Figure 7(b) showed strongly damaged steel surface due to the formation of corrosion products after immersion in SCPS. SEM images of steel surface after immersion in 250 ppm lactic acid and 50 ppm Zn^{2+} are shown in Figure 7(c).

The SEM micrograph (×1000) of Figure 7(a) shows the smooth surface of mild steel without any corrosion product or inhibitor complex on the metal surface. Inspection of Figure 7(b) reveals that the mild steel immersed in SCPS shows an aggressive attack of the corroding medium on the steel surface. In contrast, in the presence of 250 ppm lactic acid and 50 ppm Zn^{2+} the mild steel surface coverage increses which in turn results in the formation of insoluble complex on the metal surface (LA + Zn inhibitor complex) [30–33].
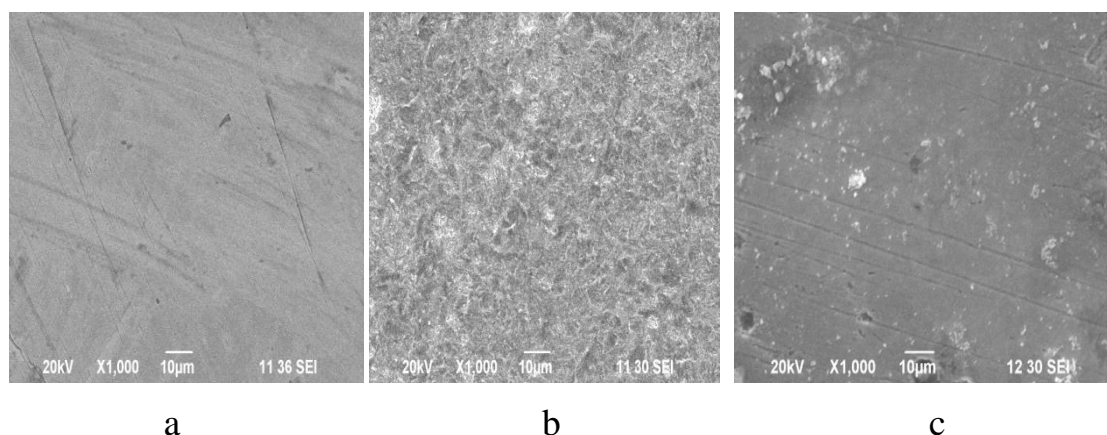

a   b   c

Figure 7. SEM micrographs of (a) mild steel; magnification ×1000; (b) mild steel immersed in SCPS prepared in well water; magnification ×1000; (c) mild steel immersed in SCPS prepared in well water containing LA (250 ppm) + Zn^{2+} (50 ppm); magnification ×1000.

Atomic Force Microscopy Characterization

Atomic Force Microscopy (AFM Analysis) provides images with atomic or near-atomic-resolution surface topography, capable of quantifying surface roughness of samples down to the angstrom-scale. Atomic force microscopy (AFM) or scanning force microscopy (SFM) is a very higher resolution type of scanning probe microscopy, with demonstrated resolution on the order of fractions of a nanometer, more than 1000 times better than the optical diffraction limit [21]. The three dimensional (3D) AFM morphologies and the AFM cross-sectional profile for polished carbon steel surface (reference sample), carbon steel surface immersed in SCPS (blank sample) and carbon steel surface immersed in SCPS containing the formulation of 250 ppm of LA and 50 ppm of Zn^{2+} are shown as Figure 8 images (a, d), (b, e), (c, f) respectively [34, 35].

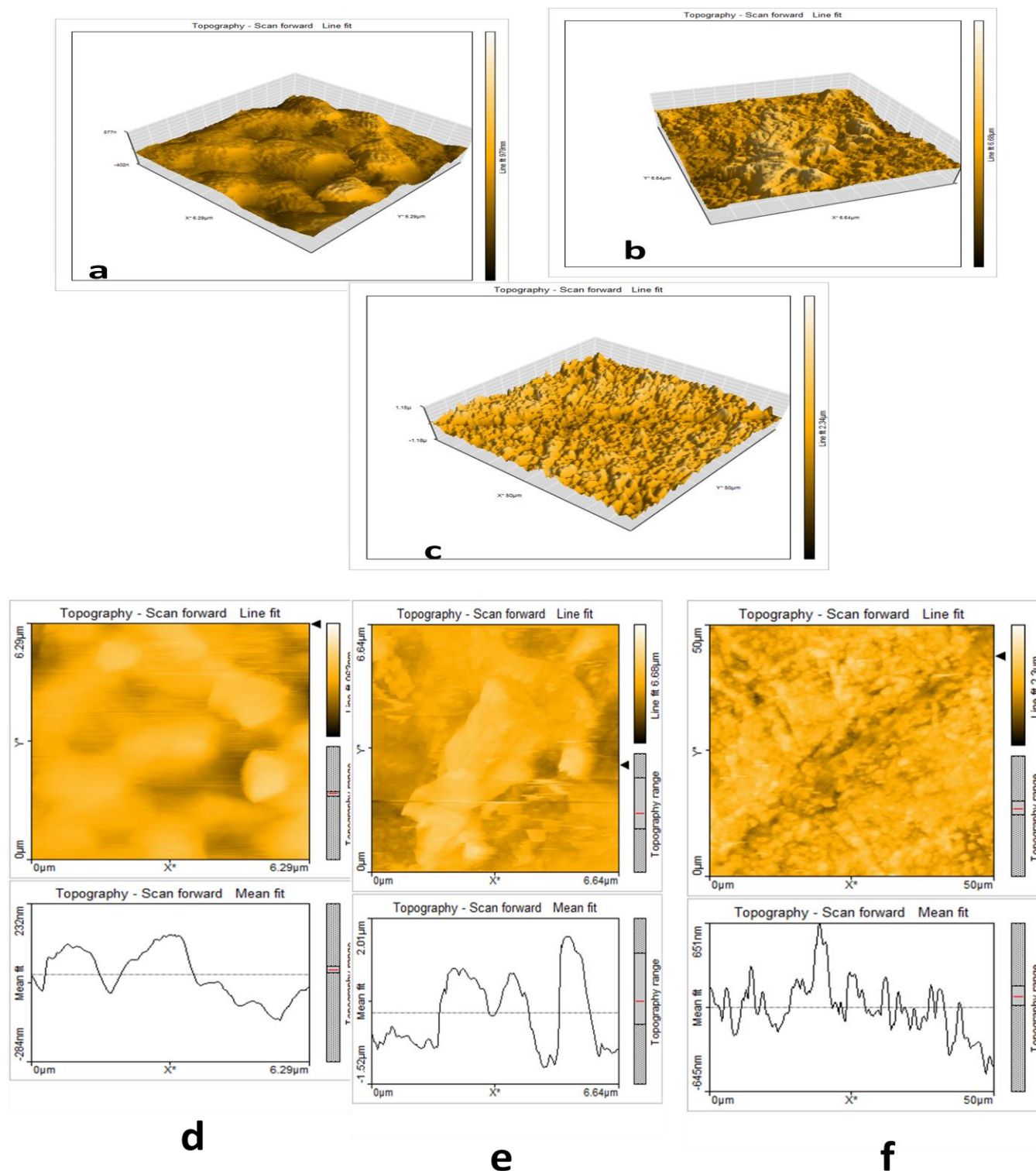*Int. J. Corros. Scale Inhib.*, 2017, **6**, no. 1, 18–31

28

Figure 8. (a,b,c). Three dimensional AFM images of the surface of: a) As polished carbon steel (control); b) carbon steel immersed in SCPS (blank); c) carbon steel immersed in SCPS containing LA (250 ppm) + Zn^{2+} (50 ppm); (d,e,f). AFM cross-sectional images of the surface of: d) as polished carbon steel (control); e) carbon steel immersed in SCPS (blank); f) carbon steel immersed in SCPS containing LA (250 ppm) + Zn^{2+} (50 ppm).

Root-mean-square roughness, average roughness and peak-to-valley value AFM image analysis was performed to obtain the average roughness, R_a (the average deviation of all points roughness profile from a mean line over the evaluation length), root-mean-square roughness, R_q (the average of the measured height deviations taken within the evaluation length and measured from the mean line) and the maximum peak-to-valley (P−V) height values (largest single peak-to-valley height in five adjoining sampling heights). Table 5 is a summary of (R_q), (R_a), (P−V) values for carbon steel surface immersed in different environments.

Table 5. AFM data for carbon steel surface immersed in inhibited and uninhibited environment.

Samples	RMS (R_q) Roughness (nm)	Average (R_a) Roughness (nm)	Maximum peak-to-peak height (nm)
Polished mild steel (Control)	3.53	4.36	5.89
Mild steel immersed in SCPS	87.90	264.86	303.90
Mild steel immersed in SCPS + lactic acid 250 ppm + Zn^{2+} 50 ppm	35.52	41.14	93.45

Figure 8 (a, d) displays the surface topography of un-corroded metal surface. The value of R_q, R_a and P−V height for the polished carbon steel surface (reference sample) are 3.53 nm, 4.36 nm and 5.89 nm respectively. The slight roughness observed on the polished carbon steel surface is due to atmospheric corrosion. Figure 8 (b, e) displays the corroded metal surface with few pits in the absence of the inhibitor immersed in SCPS. The R_q, R_a, P−V height values for the carbon steel surface are 87.90 nm, 264.86 nm and 303.90 nm respectively. These data suggests that carbon steel surface immersed in SCPS has a greater surface roughness than the polished metal surface, which shows that the unprotected carbon steel surface is rougher and was due to the corrosion of the carbon steel in dam water environment. Figure 8(c, f) displays the steel surface after immersion in sea water containing 250 ppm of LA and 50 ppm of Zn^{2+}. The R_q, R_a, P−V height values for the carbon steel surface are 135.52 nm, 41.14 nm and 93.45 nm respectively. The R_q, R_a, P−V height values are considerably less in the inhibited environment compared to the uninhibited environment. These parameters confirm that the surface is smoother. The smoothness of the surface is due to the formation of a compact protective film of Fe^{2+}−LA complex and $Zn(OH)_2$ on the metal surface there by inhibiting the corrosion of carbon steel [34, 35].

Acknowledgement

Conclusion

The present study leads to the following conclusions:

i. The formulation consisting of 250 ppm of lactic acid and 50 ppm of Zn^{2+} offers 94% *IE* to mild steel immersed in simulated concrete pore solution prepared in well water.
ii. Polarization study reveals that lactic acid system controls the anodic reaction predominantly.
iii. AC impedance spectra reveal that the formation of protective film on the metal surface.
iv. FTIR spectra reveal that the inhibitive film consists of Fe^{2+}–lactic acid complex, calcium carbonate, calcium oxide and calcium hydroxide.
v. SEM and AFM images confirmed the protective film formed on the metal surface was smooth and stable.

References

1. L. Bertonoli, B. Elsener, P. Pedeferi and R. Polder, *Corrosion of Steel in Concrete: Prevention, Diagnosis, Repair*, Wiley, Weinhein, 2004.
2. C.L. Page, *Nature and Properties of Concrete in Relation to Reinforcement Corrosion. Corrosion of steel in Concrete*, Aachen, 1992.
3. B. Elsener, *Corrosion Inhibitors for steel in Concrete – State of the Art Report, EFC Publications*, Vol. 35, 2001.
4. N.S. Berke, *Mater. Perform.*, 1989, **23**, no. 10, 41.
5. N.S. Berke and T.G. Weil, *World-wide Review of Corrosion Inhibitors in Concrete; Advances in Concrete Technology*, CANMET, 1992, Athen, Greece, pp. 899–924.
6. R. Cigna, G. Familiari, F. Gianetti and E. Proverbio, *International Conference on Corrosion and Corrosion Protection of steel in Concrete*, 1994, Sheffild, 878.
7. I. Callander and A. Gianetti, *A review on the use of C.N corrosion inhibitor to improve the durability of reinforced concrete*, The 2nd Annual Middle East Protection and Rehabilitation of Reinforced Concrete Conference, Dubai, 1996, 1-1.
8. N.S. Berke and M.C. Hicks, *Cem. Concr. Compos.*, 2004, **26**, 191.
9. C. Andrade, C. Alons, M. Acha and B. Malric, *Cem. Concr. Compos*, 1996, **26**, 191.
10. V.T. Nagla, C.L. Page and M.M. Page, *Corros. Sci.*, 2003, **45**, 1523.
11. D. Bejegovic, B. Miksic, *Mater. Perform*, 1999, **11**, 52.
12. O.T. de Rincon Preez, E. Paredes, Y. Caldera, C. Urdaneta and C. Sandoval, *Cem. Concr. Compos*, 2002, **24**, 79.
13. K.K. Sagoe-Crentsil, V.T. Yilmaz and F.P. Glasser, *Adv. Cem. Res.*, 1996, **4**, 91.
14. K.K. Sagoe-Crentsil, F.P. Glasser and V.T. Yilmaz, *Cem. Concr. Compos.*, 1994, **24**, 313.
15. V. Saraswathy, S. Muralidharan, R.M. Kalyanasundaram, S. Thangavel and S. Srinivasan, *Cem. Concr. Compos.*, 2001, **31**, 789.
16. R. Liu, L. Jiang, J. Xu, C. Xiong and Z. Song, *Constr. Build. Mater.*, 2014, **56**, 16.
17. M. Manivannan and S. Rajendran, *Int. J. Eng. Sci. Technol.*, 2011, **3**, 19.

18. V. Johnsirani, J. Sathiyabama, S. Rajendran, T. Shanthi, T.S. Muthumegala and A. Krishnaveni, *Bulg. Chem. Commun.*, 2012, **44**, 41.
19. R. Epshiba, A.P.P. Regis and S. Rajendran, *Int. J. Nano Corr. Sci. Eng.*, 2014, **1**, no. 1, 1.
20. N. Kavitha and P. Manjula, *Int. J. Nano Corr. Sci. Eng.*, 2014, **1**, no. 1, 31.
21. R. Nagalakshmi, L. Nagarajan, R.J. Rathish, S.S. Prabha, N. Vijaya, J. Jeyasundari and S. Rajendran, *Int. J. Nano Corr. Sci. Eng.*, 2014, **1**, no. 1, 39.
22. J. A. Thangakani, S. Rajendran, J. Sathiabam, R.M. Joany, R.J. Rathis and S.S. Prabha, *Int. J. Nano Corr. Sci. Eng.*, 2014, **1**, no. 1, 50.
23. A. Nithya, P. Shanthy, N. Vijaya, R.J. Rathish, S.S. Prabha, R.M. Joany and S. Rajendran, *Int. J. Nano Corr. Sci. Eng.*, 2015, **2**, no. 1, 1.
24. T. Gowrani, P. Manjula, C.N. Baby, K.N. Manonmani, R. Sudha and T. Vennila, *Int. J. Nano Corr. Sci. Eng.*, 2015, **2**, no. 1, 12.
27. K. Namita, K. Johar, R. Bhrara, R. Epshiba and G. Singh, *Int. J. Nano Corr. Sci. Eng.*, 2015, **2**, no. 1, 22.
25. A.C.C. Mary, S. Rajendran, H. Al-Hashem, R.J. Rathish, T. Umasankareswari and J. Jeyasundari, *Int. J. Nano Corr. Sci. Eng.*, 2015, **2**, no. 1, 42.
26. V. Johnsirani, S. Rajendran, A. C.C. Mary, R.J. Rathish, T. Umasankareswari and J. Jeyasundari, *Int. J. Nano Corr. Sci. Eng.*, 2015, **2**, no. 3, 22.
27. P.N. Devi, J. Sathiyabama, S. Rajendran, R. J. Rathish and S.S. Prabha, *Int. J. Nano Corr. Sci. Eng.*, 2015, **2**, no. 4, 1.
28. T. Shanthi and S. Rajendran, *J. Chem. Biol. Phys. Sci.*, 2013, **3**, no. 4, 2550.
29. P.N. Devi, J. Sathiyabama, S. Rajendran, R.J. Rathish and S.S. Prabha, *Int. J. Nano Corr. Sci. Eng.*, 2015, **2**, no. 3, 1.
30. D.B. Hmamou, R. Salghi, A. Zarrouk, M. Messali, H. Zarrok, M. Errami, B. Hammouti, Lh. Bazzi and A. Chakir, *Der Pharma Chemica*, 2012, **4**, no. 4, 1496.
31. M. Sangeetha, S. Rajendran, J. Sathiyabama, T. Umasankareswari, A. Krishnaveni and R.M. Joany, *Int. J. Nano Corr. Sci. Eng.*, 2015, **2**, no. 3, 14.
32. P.N. Devi, J. Sathiyabama, S. Rajendran, R.J. Rathish and D. Renita, *Int. J. Nano Corr. Sci. Eng.*, 2015, **2**, no.5, 347.
33. A.K. Singh and M.A. Quraishi, *Corros. Sci.*, 2011, **53**, no. 4, 1288.
34. M. Sangeetha, S. Rajendran, J. Sathiyabama, A. Krishnavani, N. Manimaran and B. Shamaladevi, *Port. Electrochim. Acta*, 2014, **29**, 429.
35. R. Vera, R. Schrebler, P. Cury, R. Del Rio and H. Romero, *J. Appl. Elecrochem.*, 2007, **37**, 519.

♦ ♦ ♦